PHYSICAL REVIEW D **90,** 091501(R) (2014)

# Gluon spectral functions and transport coefficients in Yang-Mills theory

Michael Haas,[1,2] Leonard Fister,[3] and Jan M. Pawlowski[1,2]

[1]*Institut für Theoretische Physik, Universität Heidelberg, Philosophenweg 16, 69120 Heidelberg, Germany*

[2]*ExtreMe Matter Institute EMMI, GSI Helmholtzzentrum für Schwerionenforschung mbH, Planckstrasse 1, D-64291 Darmstadt, Germany*

[3]*Department for Mathematical Physics, National University of Ireland Maynooth, Maynooth, Ireland*

(Received 30 October 2013; revised manuscript received 23 April 2014; published 6 November 2014)

We compute nonperturbative gluon spectral functions at finite temperature in quenched QCD with the maximum entropy method. We also provide a closed loop equation for the spectral function of the energy-momentum tensor in terms of the gluon spectral function. This setup is then used for computing the shear viscosity over entropy ratio $\eta/s$ in a temperature range from about $0.4T_c$ to $4.5T_c$. The ratio $\eta/s$ has a minimum at about $1.25T_c$ with the value of about 0.115. We also discuss extensions of the present results to QCD.

DOI: 10.1103/PhysRevD.90.091501 PACS numbers: 12.38.Aw, 11.10.Wx, 11.15.Tk

## I. INTRODUCTION

Heavy-ion collisions at RHIC (Brookhaven) revealed about a decade ago, that the quark-gluon-plasma (QGP) is well-described by hydrodynamics [1]. It was also suggested that the QGP might be close to exhibit perfect fluidity signaled by a (almost) vanishing viscosity over entropy ratio $\eta/s$. Since then, many efforts have been made to increase the insight into the dynamics of the hot plasma, for a review see [2].

The ratio $\eta/s$ has been conjectured to satisfy a universal lower bound Kovtun-Son-Starinet bound (KSS-bound) of $1/4\pi$ derived within the AdS-CFT correspondence [3]. Such a minimum can already be motivated within a quasiparticle picture: there, shear viscosity relates to a cross section, while the entropy density encodes the phase space volume of the quasiparticle. In the quasiparticle picture both quantities are related and their ratio is bounded from below.

Measurements of the elliptic flow variable $v_2$ at RHIC and CERN indeed indicate a shear viscosity to entropy ratio for the QGP which is of the order of the AdS-CFT bound [4,5]. In turn, theoretical approaches to this quantity have to face the problem that perturbation theory is not applicable in the vicinity of the confinement-deconfinement transition temperature, and for a strongly correlated plasma.

Transport coefficients can be obtained from the spectral function of the energy-momentum tensor via the Kubo relations [6]. However, most nonperturbative methods such as lattice QCD and functional continuum methods are so far limited to the computation of Euclidean correlation functions of the energy-momentum tensor, see e.g. [7–10] for lattice results. The related spectral function is then obtained via an integral equation. The latter has to be inverted from a discrete set of points, or more generally from numerical data, for example with the maximum entropy method (MEM), e.g. [11] or the Tikhonov regularization, e.g. [12]. So far, the resulting spectral functions $\rho(\omega,\vec{p})$ are subject to large statistical as well as systematical errors.

In principle, MEM and similar inversion methods are powerful tools for providing reliable spectral functions, but this requires accurate initial Euclidean correlation functions and some knowledge about their real-time asymptotics and complex structure. Whether such a situation applies directly to the correlation function of the energy-momentum tensor is difficult to answer and is part of the systematic error.

In the present work we apply MEM for the computation of the gluon spectral functions in Landau gauge Yang–Mills theory at finite temperature from Euclidean propagators obtained from Functional Renormalization Group (FRG) calculations [13]. It is well known that the gluon spectral function exhibits positivity violation, e.g. [14], and we implement an adjustment of MEM for nonpositive functions. We provide gluonic spectral functions for $0.4T_c \lesssim T \lesssim 4.5T_c$. Moreover, the zero temperature extrapolation of our results agrees well with the direct $T = 0$ computation with Dyson–Schwinger equations in [15].

The gluon spectral functions are then used to compute the viscosity over entropy ratio in this temperature range from a compact closed expression of the spectral function of the energy-momentum tensor in terms of gluon propagators and classical and full vertices.

## II. MAXIMUM ENTROPY METHOD

The spectral function $\rho(\omega,\vec{p})$ is related to the Euclidean propagator $G(i\omega_n,\vec{p})$ via the integral equation

$$G(\tau,\vec{p}) = \int_0^\infty \frac{d\omega}{2\pi} K_T(\tau,\omega)\rho(\omega,\vec{p}), \tag{1}$$

with

$$K_T(\tau,\omega) = (1+n(\omega))e^{-\omega\tau} + n(\omega)e^{\omega\tau}, \tag{2}$$

 

with thermal distribution $n(\omega) = 1/(e^{\omega/T} - 1)$. In (1), $G(\tau, \vec{p})$ denotes the Fourier transform of the Euclidean propagator $G(i\omega_n, \vec{p})$ in a slight abuse of notation.

The inversion of (1) is not unique, and it is necessary to include information on the general shape of the spectral function. That is achieved by introducing a positive model function $m(\omega, \vec{p})$, containing all available information on the asymptotic behavior (shape) of $\rho(\omega, \vec{p})$. In practice $m(\omega, \vec{p})$ encodes the correct UV behavior known from perturbation theory. MEM minimizes the quantity $Q(\vec{p}) = L(\vec{p}) - \alpha S(\vec{p})$ with

$$L(\vec{p}) = \frac{1}{2}\int_0^{\frac{\beta}{2}} \frac{d\tau}{\sigma^2(\tau, \vec{p})}(G(\tau, \vec{p}) - G_\rho(\tau, \vec{p}))^2, \quad (3)$$

and

$$S(\vec{p}) = \int_0^\infty d\omega \left[\rho(\omega, \vec{p}) - m(\omega, \vec{p}) - \rho(\omega, \vec{p}) \log \frac{\rho(\omega, \vec{p})}{m(\omega, \vec{p})}\right]. \quad (4)$$

Here $\sigma(\tau, \vec{p})$ encodes the uncertainties of the input correlator. In (3) $G_\rho(\tau, \vec{p})$ denotes the propagator calculated from the MEM spectral function via (1). The likelihood term (3) and the entropy term (4) of Shannon-Jaynes type [16] are related by the weight parameter $\alpha$. The weight parameter regulates the relative importance of the model with respect to the correlator, and can be integrated out, see e.g. [11].

For positive model functions, the MEM ansatz for the spectral function is intrinsically positive. However, the gluon spectral functions $\rho(\omega, \vec{p})$ show positivity violation for large frequencies and sufficiently low momenta. This property relates to the fact that the gluon is no asymptotic state, and is taken into account by parametrizing the spectral functions as a difference of two positive model functions: $\rho(\omega, \vec{p}) = \rho_s(\omega, \vec{p}) - s(\omega, \vec{p})$. Such splittings have been also used for, e.g., quark spectral functions, for recent work see [17]. The shift function $s(\omega, \vec{p})$ should allow for a finite violation of positivity, i.e. no poles and essential singularities. The propagator corresponding to $\rho_s(\omega, \vec{p})$ is

$$G_s(\tau, \vec{p}) = G(\tau, \vec{p}) + \Delta G(\tau, \vec{p}) \quad (5)$$

where

$$\Delta G(\tau, \vec{p}) = \int_0^\infty \frac{d\omega}{2\pi} K_T(\tau, \omega) s(\omega, \vec{p}). \quad (6)$$

The finiteness of the integral (6) is guaranteed by the known, perturbative, asymptotic behavior of $\rho(\omega, \vec{p})$. For the present calculations, a temperature depend $\omega_0$ is chosen, such that the model function is constant for $\omega \leq \omega_0$ and decays to zero above $\omega_0$ with the correct asymptotics [18]. The shift function is identical to the model function apart from the low frequency region, where the shift function is exponentially suppressed.

## III. VISCOSITY

One of the main goals of the present work is the computation of the viscosity over entropy ratio $\eta/s$ as a function of temperature in the vicinity of the phase transition temperature. With the Kubo relation the shear viscosity $\eta$ is computed from the slope of the spectral function $\rho_{\pi\pi}$ of the spatial, traceless part of the energy-momentum tensor $\pi_{ij}$ at vanishing frequency,

$$\eta = \lim_{\omega \to 0} \frac{1}{20} \frac{\rho_{\pi\pi}(\omega, \vec{0})}{\omega}, \quad (7)$$

with

$$\rho_{\pi\pi}(\omega, \vec{p}) = \int \frac{dx_0}{2\pi} \int \frac{d^3x}{(2\pi)^3} e^{-i\omega x_0 + i\vec{p}\,\vec{x}} \langle [\pi_{ij}(x), \pi_{ij}(0)] \rangle. \quad (8)$$

For the computation of (8) we use that general correlation functions can be written in terms of propagators and field derivatives, see e.g. [19],

$$\langle \pi_{ij}[A]\pi_{ij}[A] \rangle = \pi_{ij}\left[G_{A\phi_i} \cdot \frac{\delta}{\delta \bar{\phi}_i} + \bar{A}\right] \pi_{ij}\left[G_{A\phi_i} \cdot \frac{\delta}{\delta \bar{\phi}_i} + \bar{A}\right], \quad (9)$$

where $\phi = (A, C, \bar{C})$ stands for the expectation values of the fields, e.g. $\bar{A} = \langle A \rangle$, and $G_{\phi_i \phi_j} = \langle \phi_i \phi_j \rangle - \langle \phi_i \rangle \langle \phi_j \rangle$ is the propagator of the respective fields.

Equation (9) consists of a finite number of connected diagrams in full propagators. The one-particle irreducible diagrams can be divided into two classes. The first class consists of one- to three-loop diagrams with gluon propagators that simply connect one $\pi_{ij}$ with the other, see Fig. 1(a). The second class consists of diagrams that can be interpreted as effective vertex corrections of the first class. A simple example is depicted in Fig. 1(b), the full diagrammatics will be discussed elsewhere [20].

In the present work we concentrate on temperatures of the order of $T_c$. In [21] it has been discussed that higher loop corrections in such an expansion in full propagators and full and classical vertices can be minimized within an optimized renormalization group scheme (RG-scheme) for temperatures about $T_c$. Note, that even though this argument has been put forward in the context of the Polyakov loop potential, it has been applied to the effective action, that generates all correlation functions. Indeed, the explicit computation confirms that higher loop orders in Fig. 1 are suppressed at these temperatures [20]. Accordingly, the weighted difference of the full computation of the Polyakov

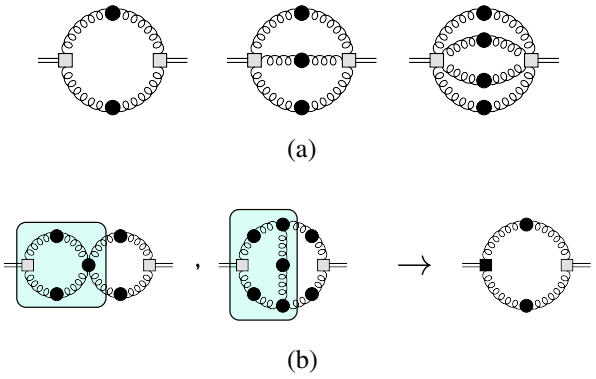

FIG. 1 (color online). Diagrams contributing to the energy-momentum tensor spectral function. (a) The three different classes of diagrams: two energy-momentum tensors (double lines) connected by 2,3,4 full internal gluon propagators. (b) Examples for effective energy-momentum tensor vertex corrections for the one-loop diagram in (a).

loop potential and the one loop computation in full propagators can be used as an estimate for the systematic error.

In conclusion, for temperatures about $T_c$ we can restrict ourselves to the one-loop contribution in Fig. 1(a). Note also, that connected contributions are of higher order and hence are dropped in the present computation. In this approximation the spectral function $\rho_{\pi\pi}$ reads

$$\rho_{\pi\pi}(p) = \mathrm{Im}\left[\int \frac{d^4k}{(2\pi)^4}\pi^{(2)}(k,p+k)G(p+k) \times \pi^{(2)}(p+k,k)G(k)\right], \tag{10}$$

where $\pi^{(2)}$ denotes the two-gluon vertex of the energy-momentum tensor $\pi$, and $p=(\omega,\vec{0})$. For the sake of brevity we omitted the color and Lorentz indices. The gluon propagators in Landau gauge at finite temperature have two separate tensor structures, longitudinal and transverse to the heat bath. For each tensor structure we have a scalar propagator $G_{L/T}(p_0^2,\vec{p}^2)$. In order to evaluate (10) we insert the tensor expression for $G(p)$ and use the cutting rules within the real-time formalism for the scalar parts of the propagators. Finally, we insert the spectral representation for the propagators. The details will be discussed in [20] and we only present the results,

$$\begin{aligned}\rho_{\pi\pi}(\omega) = \frac{2d_A}{3}\int \frac{d^4k}{(2\pi)^4}[n(k^0)-n(k^0+\omega)] \\ \times\{V_1(k,\omega)\rho_T(k^0,\vec{k})\rho_T(k^0+\omega,\vec{k}) \\ + V_2(k,\omega)\rho_T(k^0,\vec{k})\rho_L(k^0+\omega,\vec{k}) \\ + V_3(k,\omega)\rho_L(k^0,\vec{k})\rho_L(k^0+\omega,\vec{k})\},\end{aligned} \tag{11}$$

with $d_A = N_c^2-1$, and

$$\begin{aligned}V_1(k,\omega=0) &= 7(k^2)^2 - 10k_0^2\vec{k}^2 + 7k_0^4 \\ V_2(k,\omega=0) &= 6k_0^2(k_0^2-\vec{k}^2) \\ V_3(k,\omega=0) &= 2(k_0^2-\vec{k}^2)^2.\end{aligned} \tag{12}$$

The $V_i$'s are the coefficients in Landau gauge arising from the vertex contractions. If we apply the present cutting-rule approach to Coloumb gauge, the coefficients agree with that obtained in [22] from a Matsubara approach.

Equation (11) has an important feature. When taking the derivative with respect to $\omega$ at $\omega=0$, the derivative only hits the thermal distribution function. Thus, the results for the viscosity are not sensitive to the slope of the gluon spectral functions at vanishing frequency. Differentiating (8) with respect to $\omega$ at $\omega=0$ yields

$$\begin{aligned}\eta = -\frac{2d_A}{3}\int \frac{d^4k}{(2\pi)^4}n'(k^0) \\ \times\{V_1(k)\rho_T^2(k^0,\vec{k}) + V_2(k)\rho_T(k^0,\vec{k})\rho_L(k^0,\vec{k}) \\ + V_3(k)\rho_L^2(k^0,\vec{k})\}.\end{aligned} \tag{13}$$

For the computation of the viscosity over entropy ratio $\eta/s$ we take the entropy obtained within lattice calculations in [23].

## IV. RESULTS

The results are computed from the Euclidean Yang–Mills propagators at vanishing frequency $\omega_n=0$ for the longitudinal and transverse gluons for different temperatures obtained by FRG techniques, [13]. For comparison and error estimates we also utilize lattice results from [24–26], see also [27–30]. We have done this comparison for the temperature regime at about $T_c$ where the respective results agree well.

In our computations we have approximated the higher Matsubara modes in the scalar propagators $G_{L/T}$ for $\omega_n\neq 0$ with $G_{L/T}(\omega_n^2,\vec{p}^2) = G_{L/T}(0,\omega_n^2+\vec{p}^2)$. This is a quantitative approximation with a small error margin of $<1\%$, see [13], well below the systematic errors in the present computation to be discussed later.

Figure 2 shows the MEM-results for the transverse gluon spectral functions for a temperature range from $T=0.79T_c$ to $T=3.96T_c$. The common features of all calculated gluonic spectral functions are a broad maximum at $\omega/T\approx 2.0$–$3.0$ and a violation of positivity at low spatial momenta. At larger momenta, the peak smears out and approaches the line $\omega=p$, see also Fig. 3 for the transverse spectral function at $T=1.98T_c$. The fact that the (positive) peak position for fixed $\omega$ as a function of $p$ is stationary for $p\lesssim 6$ seems to be due to the negativity of the spectral function, which inhibits the bending of peak towards the main diagonal. Hence the gluon spectral functions do not show the characteristic diagonal structure of quasiparticle

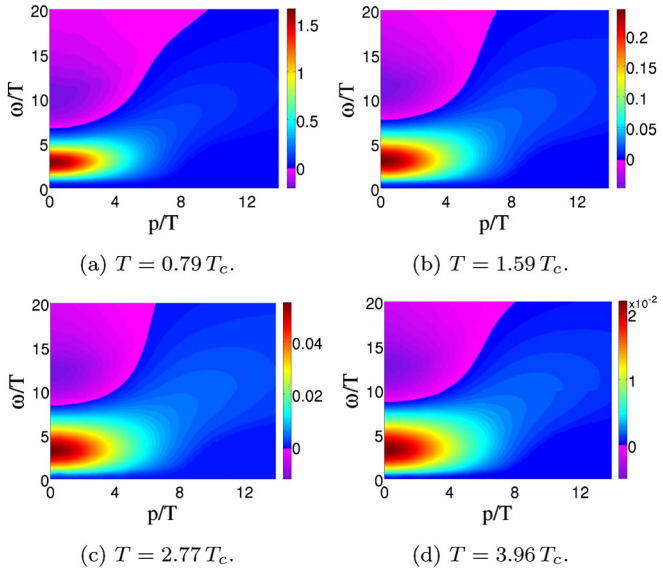


FIG. 2 (color online). Thermal dependence of transverse gluon spectrum.

spectral functions, see Fig. 3. Such a quasiparticle picture has been used e.g. in [31,32] where the model gluon spectral functions have sharper peaks with comparable peak heights.

With increasing temperature the peak broadens slightly more than linearly in $T$, while the area under the peak remains approximately constant. In the limit $T \to 0$ this would lead to a deltalike peak, as seen in [15]. The magnitude of the minimum is about 10% of the maximum of the spectral function.

The dependence of our results on the shift function is surprisingly small. We have employed different ansätze and found that only the necessary condition, that the shift function must be larger in magnitude than the negative values of the spectral function at the respective point, must be fulfilled. All other features could be chosen freely as long as (6) is kept finite. The dependence of the results on the shift function and the model function is included in the systematic MEM error, by varying both $\omega_0$ and the decay of the shift function at small frequencies. The longitudinal spectral functions show no different behavior and differ only slightly from the transverse spectral functions.

We have calculated the shear viscosity applying the Kubo relation (7) for the spectral function of the energy-momentum tensor at vanishing frequency and divided by the entropy density. In Fig. 4 we show the results as a function of temperature. The black error bars indicate the combined systematic error from both MEM computation and one-loop approximation as discussed above. In the shaded region only MEM errors are displayed. The error analysis exhibits a small systematic and statistical error for temperatures $T_c \leq T \lesssim 2T_c$. For larger temperature the one-loop approximation within the optimized RG-scheme becomes worse and higher order diagrams have to be included. In turn, for smaller temperatures $T \leq T_c$ additionally the accuracy of the spectral functions has to be increased in order to provide reliable quantitative results. Moreover, the uncertainty in the relative temperature scales on the lattice and the functional methods gets important due to the strong temperature dependence in this regime. An additional systematic error relates to the systematic error of the input data. We have also computed the ratio $\eta/s$ from the lattice propagators in [24] for temperatures about $T_c$ and the result varies with about 5%. This error is not included in the plot in Fig. 4.

The curve in Fig. 4 exhibits a clear minimum at $T = 1.25T_c$ with a value of $\eta/s = 0.115(17)$. This region is well in the regime with small systematic and statistical errors. Below the critical temperature we find a steep rise of $\eta/s$ toward lower temperatures due to the decrease of the entropy density. In view of the above error analysis this

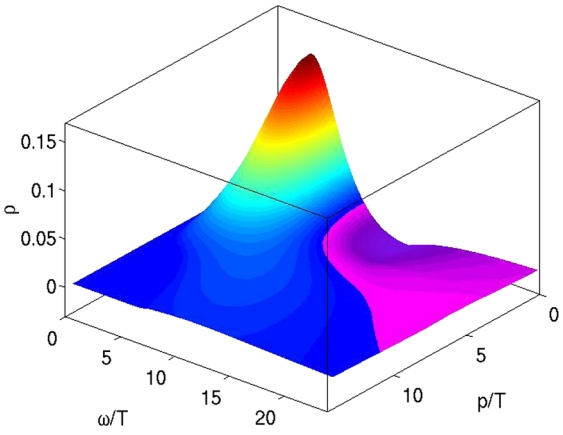


FIG. 3 (color online). Transverse gluon spectral function $\rho(\omega, \vec{p})$ for $T = 1.98T_c$.

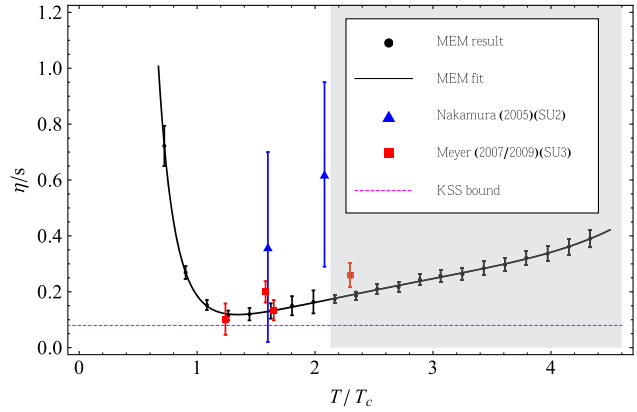


FIG. 4 (color online). Viscosity over entropy ratio $\eta/s$ for SU(3) gauge theory. The AdS/CFT bound is displayed, as well as lattice results from [9,33,34]. The black error bars indicate the combined systematic error from both MEM computation and one-loop approximation as discussed above. In the shaded region only MEM errors are displayed.

should be seen as a qualitative result. Within the present accuracy we also cannot resolve potential signatures of the first order phase transition. Our results agree qualitatively with model computations of $\eta/s$, see e.g. [35]. Note also, that for $T \leq T_c$ glueballs are expected to be the relevant degrees of freedom. It would be interesting to see how the present results fit into a corresponding quasiparticle picture based on glueballs.

## V. CONCLUSIONS

We have computed gluon spectral functions from nonperturbative, Euclidean propagators in Landau gauge finite temperature Yang–Mills theory. This has been done with a modified version of the maximum entropy method that allows for negative parts in the spectral functions. As expected the spectral functions show a violation of positivity. Our results cover the temperature regime $0.4T_c \lesssim T \lesssim 4.5T_c$. We have computed the shear viscosity $\eta$ from a closed expression in terms of the gluon spectral function. With the lattice entropy taken from [23] this leads us to the viscosity over entropy ratio $\eta/s$ in the above temperature range. We find a minimum value of $\eta/s = 0.115(17)$ at $T = 1.25T_c$ which is close to, but above the KSS bound of $\eta/s = 1/(4\pi)$. Interestingly, the results agree within the errors with previous lattice computations, [9,33]. Given the very different computational methods, this provides nontrivial support for the respective results. In [33] a mapping of Yang–Mills $\eta/s$ to QCD is proposed for $T = 2.3T_c$. Adapting the procedure we propose a minimal $\eta/s$ for QCD of 0.18. The present framework is readily extended to full QCD with dynamical fermions.

## ACKNOWLEDGMENTS

We thank N. Christiansen and N. Strodthoff for discussions and work on related subjects. This work is supported by the Helmholtz Alliance HA216/EMMI and by ERC-AdG-290623. L. F. is supported by the Science Foundation Ireland in respect of the Research Project No. 11-RFP.1-PHY3193, M. H. acknowledges support by the Landesgraduiertenförderung Baden-Württemberg via the Research Training Group "Quantum Many-body Dynamics and Nonequilibrium Physics."

[1] R. Bellwied (STAR Collaboration), arXiv:hep-ph/0112250.
[2] T. Schafer and D. Teaney, Rep. Prog. Phys. **72**, 126001 (2009).
[3] P. Kovtun, D. Son, and A. Starinets, Phys. Rev. Lett. **94**, 111601 (2005).
[4] C. Shen, U. Heinz, P. Huovinen, and H. Song, Phys. Rev. C **84**, 044903 (2011).
[5] H. Agakishiev *et al.* (STAR Collaboration), Phys. Lett. B **704**, 467 (2011).
[6] R. Kubo, J. Phys. Soc. Jpn. **12**, 570 (1957).
[7] F. Karsch and H. Wyld, Phys. Rev. D **35**, 2518 (1987).
[8] H. B. Meyer, Phys. Rev. D **76**, 101701 (2007).
[9] H. B. Meyer, Phys. Rev. Lett. **100**, 162001 (2008).
[10] H. Suganuma, T. Iritani, A. Yamamoto, and H. Iida, *Proc. Sci.*, QCD-TNT09 (2009) 044 [arXiv:0912.0437].
[11] M. Asakawa, T. Hatsuda, and Y. Nakahara, Prog. Part. Nucl. Phys. **46**, 459 (2001).
[12] D. Dudal, P. J. Silva, and O. Oliveira, *Proc. Sci.*, ConfinementX (2012) 033 [arXiv:1301.2971].
[13] L. Fister and J. M. Pawlowski, arXiv:1112.5440.
[14] A. Maas, Mod. Phys. Lett. A **20**, 1797 (2005).
[15] S. Strauss, C. S. Fischer, and C. Kellermann, Phys. Rev. Lett. **109**, 252001 (2012).
[16] E. Jaynes, Phys. Rev. **106**, 620 (1957).
[17] S.-x. Qin and D. H. Rischke, Phys. Rev. D **88**, 056007 (2013).
[18] J. M. Cornwall, Mod. Phys. Lett. A **28**, 1330035 (2013).
[19] J. M. Pawlowski, Ann. Phys. (Amsterdam) **322**, 2831 (2007).
[20] N. Christiansen, M. Haas, J. M. Pawlowski, and N. Strodthoff (to be published).
[21] L. Fister and J. M. Pawlowski, Phys. Rev. D **88**, 045010 (2013).
[22] G. Aarts and J. M. Martinez Resco, J. High Energy Phys. 04 (2002) 053.
[23] S. Borsanyi, G. Endrodi, Z. Fodor, S. Katz, and K. Szabo, J. High Energy Phys. 07 (2012) 056.
[24] C. S. Fischer, A. Maas, and J. A. Müller, Eur. Phys. J. C **68**, 165 (2010).
[25] A. Maas, Phys. Rep. **524**, 203 (2013).
[26] A. Maas, J. M. Pawlowski, L. von Smekal, and D. Spielmann, Phys. Rev. D **85**, 034037 (2012).
[27] A. Cucchieri, A. Maas, and T. Mendes, Phys. Rev. **75**, 076003 (2007).
[28] A. Cucchieri and T. Mendes, *Proc. Sci.*, FACESQCD (2010) 007 [arXiv:1105.0176].
[29] R. Aouane, V. G. Bornyakov, E.-M. Ilgenfritz, V. K. Mitrjushkin, M. Müller-Preussker, and A. Sternbeck, Phys. Rev. D **85**, 034501 (2012).
[30] A. Cucchieri and T. Mendes, *Proc. Sci.*, LATTICE2011 (2011) 206 [arXiv:1201.6086].
[31] A. Peshier, Phys. Rev. D **70**, 034016 (2004).
[32] H. Berrehrah, for the PHSD group, private communication.
[33] H. B. Meyer, Nucl. Phys. **A830**, 641C (2009).
[34] A. Nakamura and S. Sakai, Nucl. Phys. **A774**, 775 (2006).
[35] R. Marty, E. Bratkovskaya, W. Cassing, J. Aichelin, and H. Berrehrah, Phys. Rev. C **88**, 045204 (2013).